

Preparation of mesh-reinforced cellulose acetate forward osmosis membrane with very low surface roughness

Seyyed Mostafa Mirkhalili, Seyyed Abbas Mousavi[†], Ahmad Ramazani Saadat Abadi, and Masoud Sadeghi

Department of Chemical and Petroleum Engineering, Sharif University of Technology, Tehran, Iran
(Received 21 January 2017 • accepted 1 August 2017)

Abstract—Mesh-reinforced cellulose acetate (CA)-based membranes were prepared for forward osmosis (FO) by immersion precipitation. Casting compositions such as CA percent and 1, 4-dioxane/acetone ratio and also preparation conditions such as evaporation time, coagulation bath and annealing temperatures were tested for membranes' performance. The results were compared with commercially CTA membranes. The best membrane (17.9% polymer and 1, 4-dioxane/acetone ratio of 1.89) showed water flux of 9.3 L/m²h (LMH) and RSF of 0.536 mol NaCl/m²h. Moreover, the membrane structure was reinforced by a polyester mesh, which created micro pores in the back of the membrane. This caused higher water flux and RSF compared to membranes without mesh. FO membrane prepared under best conditions, had a smoother surface than commercial ones. This feature enhances the fouling properties of the membrane, which can be appropriate for wastewater treatment applications.

Keywords: Forward Osmosis, Cellulosic Membrane, Internal Concentration Polarization, Mesh-reinforced Membrane

INTRODUCTION

Forward osmosis (FO) is a membrane process that causes water to pass through a semipermeable membrane due to the osmotic pressure difference. Therefore, the difference between FO and reverse osmosis (RO) is that instead of using the hydraulic pressure, FO uses the osmotic pressure difference as the driving force [1,2]. FO has several advantages, including energy efficiency and low fouling, so it is a less expensive process in comparison with RO. Moreover, it can be economically improved if an appropriate draw solution and a good rearrangement are used [3]. Recent studies show that the power consumption of FO is not low in comparison with other desalination processes such as RO. However, FO hybrid systems, portable purifiers and desalination brine can still be good choices to use FO systems [4,5]. In addition to water desalination, FO is also used in food processing, controlled drug release, and medical product enrichment. Because of the difference between FO and RO processes, RO membranes are not appropriate for the FO process. Therefore, development of the membrane is one of the main challenges facing FO. Recent membrane developments are mainly classified in two groups: phase inversion based on cellulosic membranes and thin film composite (TFC) ones [6]. The hydrophobicity of cellulose acetate (CA) membranes and their resistance against chloride are higher than TFC membranes. Nevertheless, these membranes have low resistance against biological attacks and hydrolysis. To minimize the hydrolysis of CA membranes, pH of the feed and draw solutions should be in the range of 4-6, and the operating temperature should not exceed more than 35 °C [2].

A suitable FO membrane has a hydrophilic dense active layer with

high rate of rejection and water flux. It also has a thin and porous support layer (low internal concentration polarization (ICP)) with high mechanical strength [7]. Hence, Nguyen et al. [8] developed the FO membranes with cellulose acetate and cellulose three acetate (CTA). In their study, the effects of 1, 4-dioxane/acetone ratio, CTA/CA, casting thickness, evaporation time and annealing temperature were investigated. Their best membrane was smoother, more hydrophilic, with higher rejection and water flux compared to commercial ones. Li et al. [9] studied the effects of polymer concentration and additives of lactic acid and methanol on CTA/CA membranes. Ong et al. [10] examined the effects of different solvents on CA membranes using N-methyl-2-pyrrolidone (NMP) and 1, 4-dioxane as a solvent for CTA. They found that the membrane with NMP has higher water flux and lower rejection.

Zhang et al. [11] used casting substrates with different degrees of hydrophobicity (Teflon and glass plate) for phase inversion of cellulose acetate. By using a hydrophilic substrate in casting, a thin dense layer is created on the back of the membrane. This layer is formed by the hydrophilic-hydrophilic interaction between polymer and substrate. It also reduces loss of draw solute and then decreases ICP. Sairam et al. synthesized CA membranes with an embedded nylon mesh via phase inversion method [12]. They investigated the effects of lactic and maleic acids as well as zinc chloride with different annealing temperatures. Their results showed that ZnCl₂ mineral additives were the best pore former agents. Ahmad et al. [13] developed cellulose acetate/polyethylene glycol RO membranes. They investigated the effect of silica nanoparticles on the performance of these membranes. They showed that water flux and rejection increased with the addition of silica nanoparticles. Other researchers [14-17] studied the effects of different nanoparticles on the membrane performance, and found that nanoparticles improved the membrane properties.

There are a few studies on the synthesis of TFC membranes with a cellulose substrate [18,19]. Due to the hydrophilicity of cellulosic

[†]To whom correspondence should be addressed.

E-mail: musavi@sharif.edu

Copyright by The Korean Institute of Chemical Engineers.

Table 1. One of the combinations of HTI CA membrane [19]

Material	%
CA (cellulose acetate)	13.9
1, 4 Dioxane	53.2
Acetone	18.4
Methanol	8.2
Lactic acid	6.3

materials, polyamide layers do not form any physical bonding such as hydrophobic substrates. Therefore, a method was developed for covalent bonding of the polyamide layer with cellulosic substrates. The goal of the present study was to synthesize CA membranes. In addition, they were compared with HTI (Hydration Technology Innovations) membranes. Therefore, the combination of casting solutions was selected according to the HTI procedure (as provided in Table 1) [20]. However, as $ZnCl_2$ is a better pore former agent in comparison with lactic acid, it was used in this study [12]. Also to achieve good mechanical strength, a mesh with specific properties was used within the support layer. Then, the preparation conditions including annealing temperature, temperature of coagulation bath and the evaporation time were investigated. Finally, the effects of polymer composition and the ratio of solvents (1-4 dioxane to acetone) were studied.

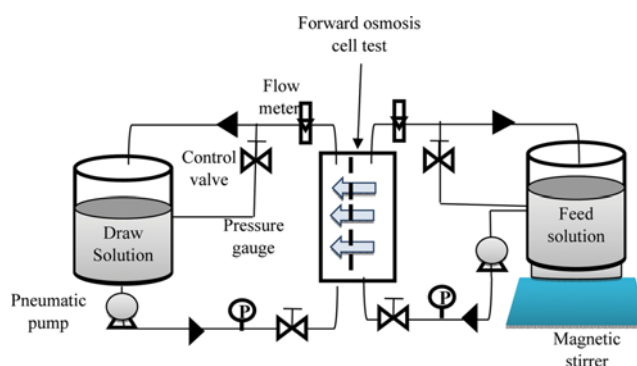
MATERIALS AND METHODS

1. Material

CA (39.8 wt% acetyl, average $M_n \approx 30,000$) with density of 1.3 g/ml was purchased from Sigma-Aldrich. 1, 4-dioxane ($\geq 99\%$ purity), acetone ($\geq 99.9\%$ purity) and zinc chloride ($ZnCl_2$, 98.0-100.5% purity) were purchased from Merck. Also, methanol ($\geq 99.8\%$ purity) and sodium chloride (NaCl, 99.0-100.5% purity) were obtained from Dr. Mojallali (Tehran, Iran). Moreover, a polyester mesh with specifications of 50 μm thickness, 31 μm mesh opening, and 21% open area was purchased from Saatile Company (Germany).

2. Preparation of Mesh-embedded CA Membrane

A homogeneous solution was prepared from the materials given in Table 1 (except that zinc chloride was used instead of lactic acid). For this purpose, the solution was stirred at a constant rate for at least 8 h. Then, the solution was cast on the mesh after 24 hours. The polymer film was then immersed in a coagulation water bath with a specified temperature. Then, the film was transferred to the second water bath at ambient temperature. Finally, the membrane was annealed for 15 minutes at a specified temperature before any

**Fig. 1. A schematic of forward osmosis performance test device.**

performance test. Also, in all of the experiments, the environmental conditions were fixed.

3. Characterization of the Membranes

3-1. FO Membrane Performance Test

Operating conditions have great effects on the performance of osmotic processes. Type and amounts of feed and draw solutions as well as temperature are some of the operating conditions which affect process efficiency. To compare different membranes, it is necessary to define a standard protocol for FO membrane performance test. Therefore, Cath et al. defined a standard methodology [21]. These operating conditions are summarized in Table 2.

FO membrane performance test device consists of a cell, a feed and a draw solution tank, two low-pressure pumps, a hydraulic pipe system with fittings and valves, two pressure gauges and two flow meters. Note that a corrosion resistant material should be used. Also, the container must be large enough to maintain the concentration of draw solution during the test. A schematic of the test device is shown in Fig. 1.

To calculate the water and reverse salt flux (RSF), volume and conductivity changes of feed solution for the period of 15 minutes were measured. Then, water and RSF were determined from Eqs. (1) and (2), respectively:

$$J_w = \frac{\Delta V}{A \cdot \Delta t} \quad (1)$$

$$J_s = \frac{C_t \cdot V_t - C_0 \cdot V_0}{A \cdot \Delta t} \quad (2)$$

where, ΔV is the volume change of the feed solution, A is the effective membrane area, C_t and C_0 are the final and initial salt concentrations, V_t and V_0 are the final and initial feed solution volumes and Δt is the time elapsed [22].

Table 2. Operating conditions of FO membrane performance test [20]

Operating conditions	Value	Notes
Feed and draw solution temperature	20 °C	-
Draw solution concentration	1 M NaCl	58.44 g/L NaCl
Feed concentration	0 M NaCl	Deionized water
Feed and draw solution cross-flow velocity	0.25 m/s	No spacer in the feed and draw solution channel, Co-current flow
Feed and draw solution pressure	<0.2 (3) bar (psi)	Low pressure as much as possible and equal on both sides of the membrane

3-2. Determination of the Intrinsic Properties of Osmotic Membranes

The water (A) and salt (B) permeability coefficients, and structure parameters (S) were calculated by the method of Tiraferri et al. [23]. This method estimates A, B and S for the osmotic membranes by using several concentrations of draw solution in the FO membrane performance test. The membranes were tested in FO mode and all the experiments were carried out in four stages. Also, each stage used different draw solution concentrations (300, 600, 900 and 1,200 mM) with distilled water as the feed solution. The water flux (J_w) and RSF (J_s) were calculated at each stage. Finally, A, B and S were obtained using the FO transport equations (Eqs. (3) and (4)) via least square regression analysis.

$$J_w = A \frac{\pi_{D,s} \exp\left(-\frac{J_w S}{D}\right) - \pi_{F,b} \exp\left(\frac{J_w}{k}\right)}{1 + \left(\frac{B}{J_w}\right) \left[\exp\left(\frac{J_w}{k}\right) - \exp\left(-\frac{J_w S}{D}\right) \right]} \quad (3)$$

$$J_s = B \frac{c_{D,s} \exp\left(-\frac{J_w S}{D}\right) - c_{F,b} \exp\left(\frac{J_w}{k}\right)}{1 + \left(\frac{B}{J_w}\right) \left[\exp\left(\frac{J_w}{k}\right) - \exp\left(-\frac{J_w S}{D}\right) \right]} \quad (4)$$

where, π_D and π_F are the osmotic pressures for the draw and feed

solutions, c_D and c_F are the concentrations of the draw and feed solutions, and D and k are draw solute bulk diffusion and feed solute mass transfer coefficients, respectively.

3-3. Viscosity Test

The viscosity of casting solutions was obtained by an Anton Paar rheometer (MCR301 model) at applied shear rates of 0.001-100 L/s at 25 °C.

3-4. Scanning Electron Microscopy (SEM) Analysis and Measuring the Thickness of the Membranes

Bottom surface of the membrane was imaged by SEM (TEFCAN VEGA II) manufactured in the Czech Republic. Membrane thickness was calculated by a manual micrometer. It was measured at five different positions and the average value was reported.

3-5. Atomic Force Microscopy (AFM) Analysis

The morphology of the membrane surface was obtained by AFM analysis (VME BUALSCOPE C-26, Denmark).

RESULTS AND DISCUSSION

1. The Effect of Different Preparation Conditions on the Membrane Performance

1-1. Effect of Annealing Temperature

Membranes with annealing temperatures of 50, 70, 80 and 90 °C were fabricated at evaporation time of 30 s and coagulation bath

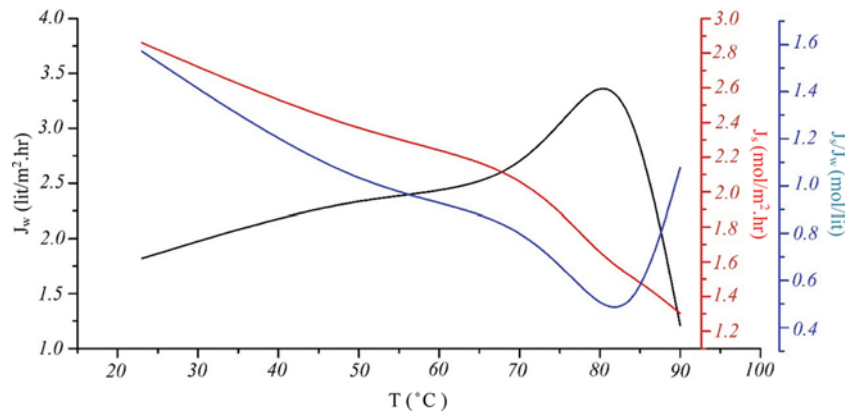


Fig. 2. Effect of annealing temperature on the performance of FO membrane (evaporation time 30 s and coagulation bath temperature 12 °C).

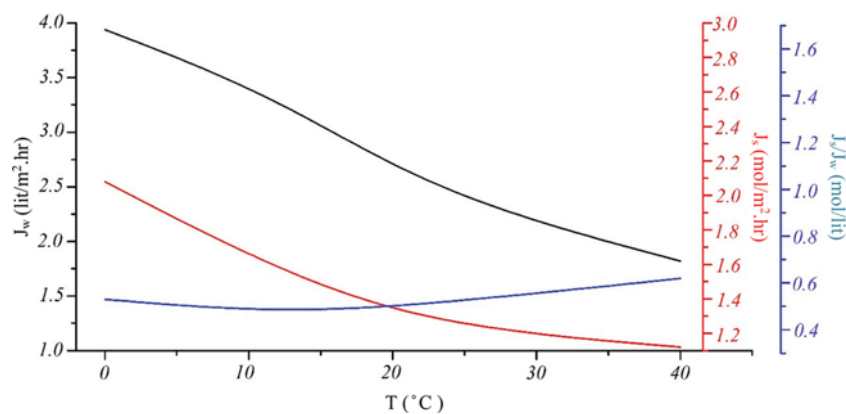


Fig. 3. Effect of coagulation bath temperature on the performance of FO membrane (evaporation time: 30 s, annealing temperature: 80 °C).

temperature of 12 °C [8,9]. Fig. 2 shows the results of the performance test for these membranes. According to the aforementioned studies [8], annealing adds thermal energy to the membrane and, therefore, hydrogen bonds increase between polymer chains. Consequently, with increasing of annealing temperature both of water flux and RSF decreased. However, at lower annealing temperatures due to exit of extra material trapped in the pores of membrane, the water flux increased and then decreased. Specific RSF which shows the membrane efficiency and selectivity is indicated in Fig. 2. This parameter was defined as the ratio of RSF to water flux. Therefore, the membrane efficiency is higher at lower specific RSF and the most suitable annealing temperature is 80 °C.

1-2. Effect of Coagulation Bath Temperature

Membranes with different coagulation bath temperatures of 0, 12, 23 and 40 °C were made at an evaporation time of 30 s and annealing temperature of 80 °C. Results of the performance test for these membranes are shown in Fig. 3. It can be seen that by increasing the coagulation temperature, both of the water flux and RSF reduced. On one hand, due to the formation of large pores the displacement speed of solvent and non-solvent increases in phase inversion process. On the other hand, as a result of the quick motion of the polymer chains their rearrangement is inhibited on the membrane surface before complete fixing by gelation or classification [9]. That is why, despite the increase in membrane porosity, water flux decreases. Therefore, the most suitable temperature for the coagulation bath is 12 °C.

1-3. The Effect of Evaporation Time

The most appropriate coagulation bath and annealing temperatures were obtained in two previous parts. Consequently, in the coagulation bath temperature of 80 °C and annealing temperature of 12 °C membranes with different evaporation times of 30, 60 and 90 s were fabricated. Fig. 4 shows the results of the performance test for these membranes. With increasing evaporation time, both water flux and RSF first increased and then decreased. According to the literature [8], since the acetone evaporated in the beginning,

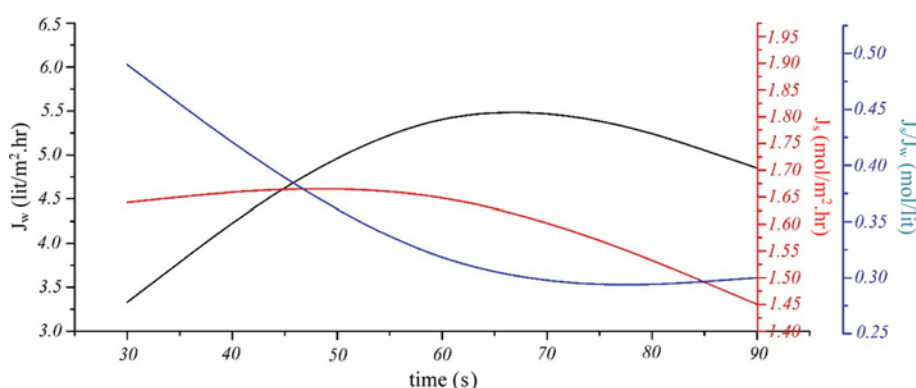


Fig. 4. Effect of evaporation time on the performance of FO membrane (coagulation bath temperature: 12 °C, annealing temperature: 80 °C).

Table 3. Comparing the results of commercial HTI membranes and this work

Membrane	Membrane thickness (μm)	Water flux (J_w) ($\text{L}/\text{m}^2 \cdot \text{hr}$)	RSF (J_s) ($\text{mol}/\text{m}^2 \cdot \text{h}$)	J_s/J_w (mol/L)
HTI-CTA [22]	97	10	0.11	0.01
This work	85-90	6.06	1.70	0.28

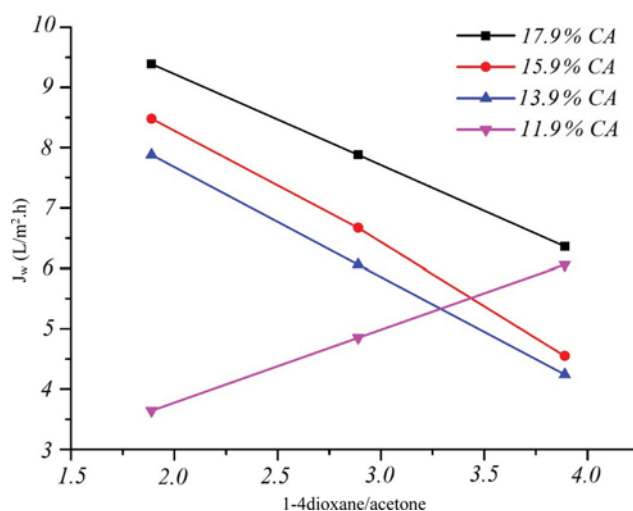


Fig. 5. The water flux in various CA concentrations and 1-4dioxane to acetone ratios.

holes were formed on the membrane surface. Therefore, both the water flux and RSF increased. However, at higher evaporation times the active layer was thicker and water flux and RSF were reduced. Furthermore, according to the specific RSF, the most appropriate evaporation time is 60 s.

2. Evaluation of Casting Composition on Membrane Performance

The comparison of the present results and commercial HTI membranes is given in Table 3. The water flux and RSF differ from each other for the two membranes. The prepared membranes show less water flux and more RSF. Therefore, it is necessary to modify the composition of casting solution in order to improve the membrane performance.

The spongy structure of the substrate increased with the increase of the percentage of polymer in casting solution. Also, the increase

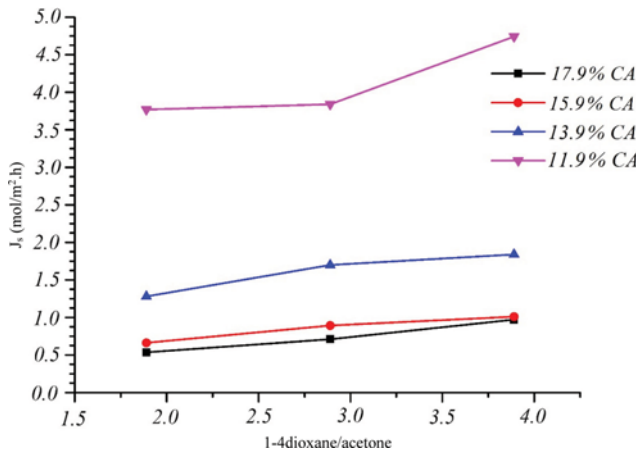


Fig. 6. RSF in various CA concentration and 1-4dioxane to acetone ratio.

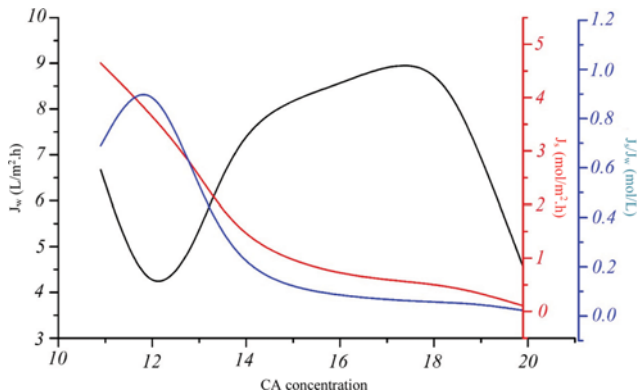


Fig. 7. The effect of CA concentration on the membrane performance at 1-4dioxane to acetone ratio of 1.89.

of acetone fraction enhanced the thickness of the active layer. Therefore, both of these factors decreased RSF. Figs. 5 and 6 show the water flux and RSF for various polymer percentages and 1-4 dioxane/acetone ratios. As can be seen, with increasing of polymer concentration, RSF decreases and water flux increases. However, it is expected that water flux is reduced as the polymer concentration increases. This unusual behavior can be explained with the reduction of acetone in the solution at higher polymer concentrations, and this may lead to the formation of an active layer. Moreover, high and low concentrations of polymer were investigated and the results are depicted in Fig. 7. Water flux is higher at very low concentrations and then decreases with increasing of polymer concentration. The reason is that by increasing of the polymer concentration in the casting solution, the spongy structure of the support layer increases [8-10]. Then, with more increasing of polymer concentration, the acetone fraction decreases in casting composition, which causes thinner active layers to be formed, and as a result water flux increases. Finally, at higher polymer concentrations, increasing of the spongy structure of the support layer compensates the effect of decreasing of active layer thickness, and so water flux is decreased. Also, RSF decreased uniformly with increasing of the polymer concentration.

Table 4. Hansen solubility parameter at 25 °C

Components	Solubility parameter (MPa) ^{0.5}
Cellulose acetate	19.56
Acetone	20.10
1-4Dioxane	20.50

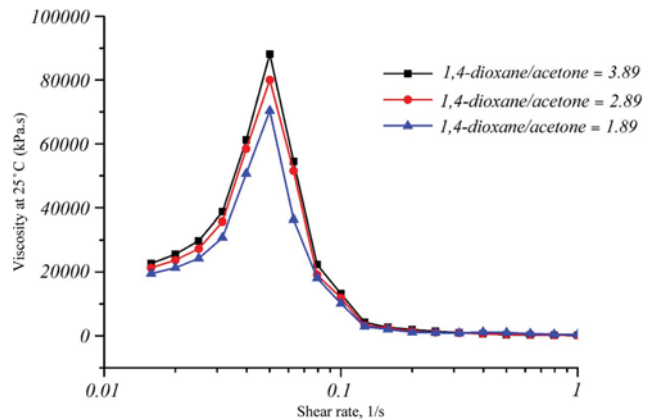


Fig. 8. The effect of different 1-4 dioxane/acetone ratios on the viscosity of solution.

As Figs. 5 and 6 show, increasing of 1-4dioxane to acetone ratio decreases the water flux and increases RSF. However, at the polymer percentage of 11.9, by increasing of this ratio both water flux and RSF increase. The presence of acetone in the casting solution may explain this phenomenon. Acetone thickens the active layer and presence of less acetone should increase water flux and RSF. However, at polymer concentrations higher than 11.9%, the RSF continues to increase while the water flux decreases. This is due to the effect of solution viscosity on the membrane structure. The miscibility of polymer increases with increasing of acetone mole fraction, and thereby a more diluted solution is formed. Hansen solubility parameters for cellulose acetate, acetone and 1-4dioxane are shown in Table 4. The miscibility of polymers with a closer solubility parameter to the solvents is higher. Therefore, the viscosity of the solution decreases as in the case of acetone. Fig. 8 shows the viscosity of 13.9% CA solution for various 1-4dioxane to acetone ratios at 25 °C. Viscosity increases with increasing of 1-4dioxane to acetone ratio. As a result, the speed of solvent and non-solvent displacement reduces and smaller pores are formed in the support layer structure. Thus, the spongy structure of the support layer increases. Therefore, water flux should be reduced in the spongy structure membranes. SEM images proved the decline in water flux with the reduction of acetone in 11.9% CA membranes. Fig. 9 shows SEM images of membrane bottom surface. These images show that polyester mesh created micro pores in the back of the membrane. These pores are affected by the polymer percentage and 1-4dioxane to acetone ratios. The number and sizes of the pores increase at low 1-4dioxane to acetone ratio and high polymer concentrations. Water flux decline is the result of the smaller number of these pores at high 1-4dioxane to acetone ratio.

For further investigation of the mesh effect on the structure, free-mesh membranes were made. Results of the performance test

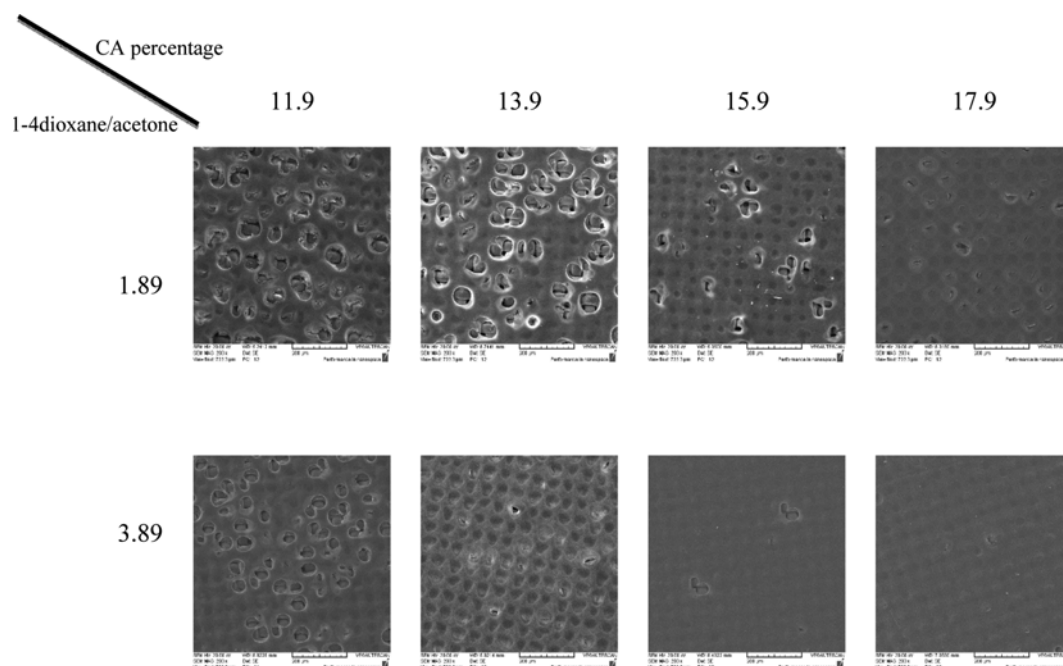


Fig. 9. SEM images of the bottom membranes in various CA percentages and 1-4 dioxane/acetone ratios.

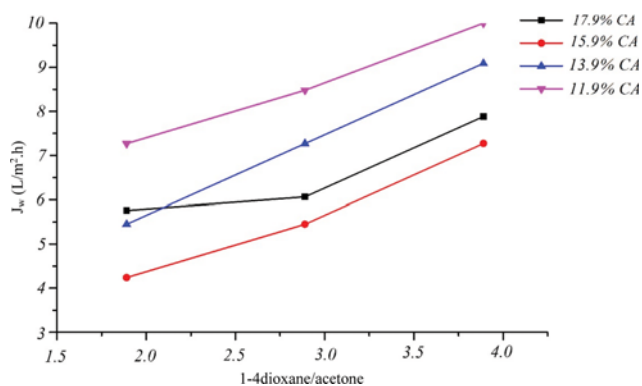


Fig. 10. Water flux in various percentages of CA and 1-4dioxane to acetone ratios for membranes without mesh.

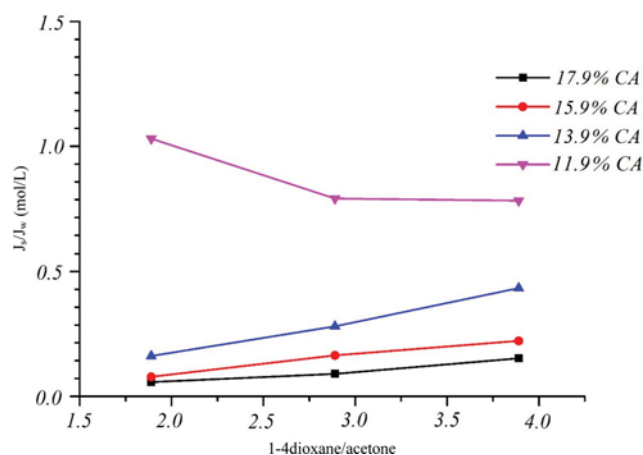


Fig. 12. Specific reverse solute flux in various percentages of CA and 1-4dioxane to acetone ratios.

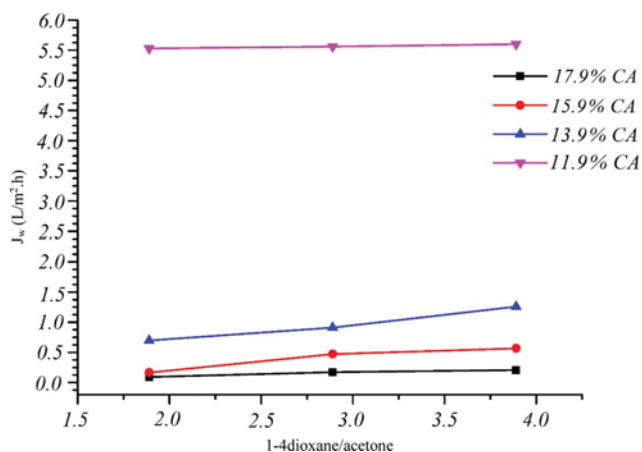


Fig. 11. RSF in various percentages of CA and 1-4dioxane to acetone ratios for membranes without mesh.

for these membranes are shown in Figs. 10 and 11. Both water flux and RSF increased with the increase of 1-4dioxane to acetone ratio. Therefore, it confirms the mesh effect on the membrane structure at different percentages of CA. Also, due to the absence of pores in the back of free-mesh membranes, their water flux and RSF were less than the mesh reinforced membranes.

Specific RSF at various CA percentages and 1-4dioxane to acetone ratios are indicated in Fig. 12. Except for membrane with 11.9% CA, reducing the percentage of acetone reduces the specific RSF. As acetone is volatile, its reduction causes less solvent to evaporate from the surface and thereby reduces the thickness of the active layer. Therefore, membrane selectivity reduces and membranes with more polymer percentage (17.9%) and less 1-4 dioxane/acetone ratio (1.89) have higher selectivity. Membranes with

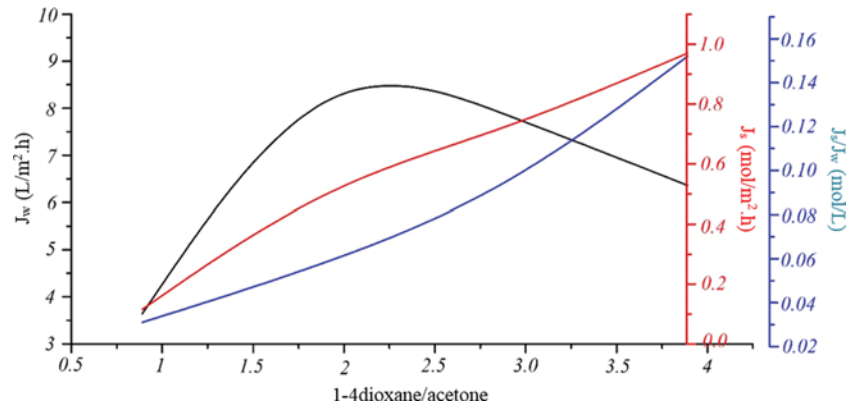


Fig. 13. Effect of various 1-4dioxane to acetone ratios on water flux.

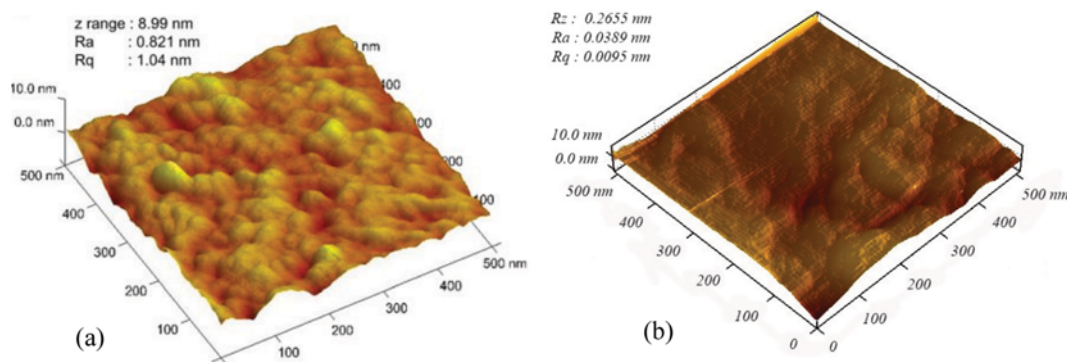


Fig. 14. AFM Images (a). Commercial HTI membrane [14] (b). The present membrane.

Table 5. Comparison of test results of HTI membrane performance and the most suitable membrane of the present research

Membrane	Membrane thickness (μm)	Water flux (J_w) ($\text{L}/\text{m}^2\cdot\text{h}$)	RSF (J_s) ($\text{mol}/\text{m}^2\cdot\text{h}$)	J_s/J_w (mol/L)	A ($\text{L}/\text{m}^2\cdot\text{h}\cdot\text{bar}$)	B ($\text{L}/\text{m}^2\cdot\text{h}$)	S (μm)
HTI-CTA	97	10	0.11	0.01	0.46	0.26	327
Appropriate membrane	85-90	9.30	0.536	0.057	0.584	0.44	464

more CA percentage and less 1-4dioxane to acetone ratio were selected as the optimum ones. For further investigation of 1-4dioxane to acetone ratios, a membrane with 1-4dioxane to acetone ratio of 0.89 was prepared. The performance test results for the membrane containing 17.9% of CA are shown in Fig. 13. Both RSF and water flux are extremely decreased. As the percentage of volatile solvent is very high in the polymer solution, a thick active layer is formed. Thus, 1.89 was selected as the best 1-4 dioxane to acetone ratio.

AFM was performed to investigate the surface properties of the membranes. Fig. 14 compares the AFM image of the best membrane (17.9% CA and 1-4dioxane to acetone ratio of 1.89) with the commercial HTI membrane. The fabricated membrane has a smoother surface in comparison with HTI one. This can be explained by the existence of mesh with less porosity and more casting solution concentration compared with the commercial HTI membrane. To have a better understanding of the morphology of the membrane surface, various parameters were defined. The average (R_a) and root mean square roughness (R_q) and the difference

between the highest peak and shortest valley (R_z) are the most commonly used parameters (and are compared in Fig. 14). This figure proves the smoother surface of the fabricated membrane in comparison with the HTI one. Also, this feature reduces the fouling on the membrane, which could be suitable for wastewater treatment applications [24].

Finally, the most appropriate membrane of this study and commercial HTI one are compared in Table 5. The results are almost similar. The remarkable thing is that water permeability of our best membrane is more than HTI one, although it has lower water flux. This can be explained by a higher structural parameters (S) of our best membrane support layer in comparison with HTI one.

CONCLUSIONS

Mesh-reinforced cellulose acetate (CA)-based membranes were prepared for forward osmosis (FO) by immersion precipitation. First, by considering the casting composition of commercial HTI membranes, preparation conditions were investigated. The evapo-

ration time of 60 s, coagulation bath temperature of 12 °C and annealing temperature of 80 °C were selected as the most suitable conditions. By comparing the results of the appropriate membrane with the commercial HTI one, it was found that significant differences exist between the two membranes. Next, preparation conditions were investigated to improve the performance of the membrane. In this section, 17.9% of CA and 1-4dioxane to acetone ratio of 1.89 were selected as the best preparation conditions. This membrane has a water flux of 9.3 LMH and RSF of 0.536 mol NaCl/m²·h. AFM analysis showed that the best fabricated membrane has a smoother surface than commercial ones. This feature enhances the fouling properties of the membranes, which can be appropriate for wastewater treatment applications.

ACKNOWLEDGEMENTS

This research was supported by the center of membrane technology at Sharif University of Technology.

SUPPORTING INFORMATION

Additional information as noted in the text. This information is available via the Internet at <http://www.springer.com/chemistry/journal/11814>.

REFERENCES

1. T. Y. Cath, A. E. Childress and M. Elimelech, *J. Membr. Sci.*, **281**, 70 (2006).
2. S. Zhao, L. Zou, C. Y. Tang and D. Mulcahy, *J. Membr. Sci.*, **396**, 1 (2012).
3. T.-S. Chung, S. Zhang, K. Y. Wang, J. Su and M. M. Ling, *Desalination*, **287**, 78 (2012).
4. R. K. McGovern and J. H. Lienhard V, *J. Membr. Sci.*, **469**, 245 (2014).
5. D. L. Shaffer, J. R. Werber, H. Jaramillo, S. Lin and M. Elimelech, *Desalination*, **356**, 271 (2015).
6. I. L. Alsvik and M.-B. Hägg, *Polymers*, **5**, 303 (2013).
7. C. Bae, K. Park, H. Heo and D.-R. Yang, *Korean J. Chem. Eng.*, **34**, 844 (2017).
8. T. P. N. Nguyen, E.-T. Yun, I.-C. Kim and Y.-N. Kwon, *J. Membr. Sci.*, **433**, 49 (2013).
9. G. Li, X.-M. Li, T. He, B. Jiang and C. Gao, *Desalin. Water. Treat.*, **51**, 2656 (2013).
10. R. C. Ong and T.-S. Chung, *J. Membr. Sci.*, **394**, 230 (2012).
11. S. Zhang, K. Y. Wang, T.-S. Chung, H. Chen, Y. C. Jean and G. Amy, *J. Membr. Sci.*, **360**, 522 (2010).
12. M. Sairam, E. Sereewatthanawut, K. Li, A. Bismarck and A. G. Livingston, *Desalination*, **273**, 299 (2011).
13. A. Ahmad, S. Waheed, S. M. Khan, S. e-Gul, M. Shafiq, M. Farooq, K. Sanaullah and T. Jamil, *Desalination*, **355**, 1 (2015).
14. W. Chen, Y. Su, L. Zhang, Q. Shi, J. Peng and Z. Jiang, *J. Membr. Sci.*, **348**, 75 (2010).
15. A. L. Ahmad, Z. A. Jawad, S. C. Low and S. H. S. Zein, *J. Membr. Sci.*, **451**, 55 (2014).
16. N. El Badawi, A. R. Ramadan, A. M. K. Esawi and M. El-Morsi, *Desalination*, **344**, 79 (2014).
17. S. Waheed, A. Ahmad, S. M. Khan, S.-e. Gul, T. Jamil, A. Islam and T. Hussain, *Desalination*, **351**, 59 (2014).
18. I. L. Alsvik and M.-B. Hägg, *J. Membr. Sci.*, **428**, 225 (2013).
19. I. L. Alsvik, K. R. Zodrow, M. Elimelech and M.-B. Hägg, *Desalination*, **312**, 2 (2013).
20. J. Herron, US Patent, 11,101,691 (2006).
21. T. Y. Cath, M. Elimelech, J. R. McCutcheon, R. L. McGinnis, A. Achilli, D. Anastasio, A. R. Brady and A. E. Childress, *Desalination*, **312**, 31 (2013).
22. D. Stillman, L. Krupp and Y.-H. La, *J. Membr. Sci.*, **468**, 308 (2014).
23. A. Tiraferri, N. Y. Yip, A. P. Straub, S. Romero-Vargas Castrillon and M. Elimelech, *J. Membr. Sci.*, **444**, 523 (2013).
24. S. Javdaneh, M. R. Mehrnia and M. Homayoonfal, *Korean J. Chem. Eng.*, **33**, 3184 (2016).

Supporting Information

Preparation of mesh-reinforced cellulose acetate forward osmosis membrane with very low surface roughness

Seyyed Mostafa Mirkhalili, Seyyed Abbas Mousavi[†], Ahmad Ramazani Saadat Abadi, and Masoud Sadeghi

Department of Chemical and Petroleum Engineering, Sharif University of Technology, Tehran, Iran

(Received 21 January 2017 • accepted 1 August 2017)

Table S1. Data of FO membrane performance test at different annealing temperatures (evaporation time 30 s and the coagulation bath temperature 12 °C)

Annealing temperature (°C)	Water flux (J_w) (L/m ² ·h)	RSF (J_s) (mol/m ² ·h)	J_s/J_w (mol/L)
23	1.82	2.86	1.57
50	2.42	2.32	0.96
70	2.82	2.17	0.89
80	3.64	1.62	0.45
85	3.03	1.49	0.49
90	1.82	1.30	1.07

Table S3. Data of FO membrane performance test at different evaporation times (coagulation bath temperature: 12 °C, annealing temperature: 80 °C)

Evaporation time (s)	Water flux (J_w) (L/m ² ·h)	RSF (J_s) (mol/m ² ·h)	J_s/J_w (mol/L)
30	3.33	1.64	0.49
60	6.06	1.70	0.28
90	4.85	1.45	0.30

Table S2. Data of FO membrane performance test at different coagulation bath temperatures (evaporation time: 30 s, annealing temperature: 80 °C)

Coagulation bath temperature (°C)	Water flux (J_w) (L/m ² ·h)	RSF (J_s) (mol/m ² ·h)	J_s/J_w (mol/L)
40	1.82	1.12	0.62
23	2.42	1.25	0.51
12	3.33	1.56	0.47
0	3.94	2.08	0.53